Biogeosciences
Discussions

Open Access

EGU

1 **Colloid-bound and dissolved phosphorus species in topsoil water extracts along a grassland**

2 **transect from Cambisol to Stagnosol**

3 Xiaoqian Jiang[1], Roland Bol[1], Barbara J. Cade-Menun[2*], Volker Nischwitz[3], Sabine Willbold[3], Sara L.

4 Bauke[4], Harry Vereecken[1], Wulf Amelung[1,4], Erwin Klumpp[1]

5 [1] Institute of Bio- and Geosciences, Agrosphere Institute (IBG-3), Forschungszentrum Jülich GmbH,

6 Jülich, Germany

7 [2] Swift Current Research and Development Centre, Agriculture and Agri-Food Canada, Box 1030, 1

8 Airport Rd. Swift Current, SK, S9H 3X2 Canada

9 [3] Central Institute for Engineering, Electronics and Analytics, Analytics (ZEA-3), Forschungszentrum

10 Jülich GmbH, Jülich, Germany

11 [4] Institute of Crop Science and Resource Conservation, Soil Science and Soil Ecology, Nussallee 13,

12 University of Bonn, 53115 Bonn, Germany

13

14 *Corresponding author

15 Barbara J. Cade-Menun, Email: Barbara.Cade-Menun@AGR.GC.CA

16

Biogeosciences
Discussions

Open Access

EGU

17 **Abstract**

18 Stagnant water conditions may release phosphorus (P) in soil solution that was formerly bound to Fe

19 oxides. To understand which P species are potentially involved, we obtained water extracts from the

20 surface soils of a gradient from Cambisol, Stagnic Cambisol to Stagnosol from temperate grassland,

21 Germany. These were filtered to < 450 nm, and divided into three procedurally-defined fractions:

22 small-sized colloids (20-450 nm), nano-sized colloids (1-20 nm), and "dissolved P" (< 1 nm), using

23 asymmetric flow field flow fractionation (AF4), as well as filtration for solution ^{31}P-NMR

24 spectroscopy. The total P of soil water extracts increased in the order Cambisol< Stagnic Cambisol<

25 Stagnosol due to increasing contributions from the dissolved P fraction. Associations of C-Fe/Al-PO$_4$$^{3-}$

26 /pyrophosphate were absent in nano-sized (1-20 nm) colloids from the Cambisol but not in the

27 Stagnosol. The ^{31}P-NMR results indicated that this was accompanied by elevated portions of organic P

28 in the order Cambisol > Stagnic Cambisol > Stagnosol. Across all soil types, elevated proportions of

29 inositol hexakisphosphate species (e.g. *myo*-, *scyllo*-, and D-*chiro*-IHP) were associated with soil

30 mineral particles (i.e. bulk soil and small-sized soil colloids) whereas other orthophosphate monoesters

31 and phosphonates were found in the 'dissolved' P fraction. We conclude that stagnic properties affect

32 P speciation and availability by potentially releasing dissolved inorganic and ester-bound P forms as

33 well as nano-sized organic matter-Fe/Al-P colloids.

34

35 **Keywords**: colloidal phosphorus; dissolved phosphorus; field flow fractionation; ^{31}P-NMR; grassland;

36 Cambisol; Stagnosol.

37

38 **Abbreviations:** AEP, 2-Aminoethyl phosphonic acid; AF4, asymmetric flow field flow fractionation;

39 Al, aluminum; Ca, calcium; DNA, deoxyribonucleic acid; EDTA, Ethylenediaminetetraacetic; Fe, iron;

40 FFF, field flow fractionation; ICP-MS, inductively coupled plasma mass spectrometer; myo-IHP,

41 myo-inositol hexakisphosphate; N, nitrogen; NMR, nuclear magnetic resonance; OC, organic carbon;

42 OCD, organic carbon detector; OM, organic matter; PES, polyethersulfone; Pi, inorganic P species; Po,

43 organic P species; Si, silicon; UV, ultraviolet; WDCs, water dispersible colloids; WDFCs, water

44 dispersible fine colloids.

Biogeosciences
Discussions

1. Introduction

Phosphorus (P) is an essential nutrient element for plant growth and limits terrestrial ecosystem productivity in many arable and grassland soils (Vance et al., 2003). The availability and transport of P depend on the speciation and concentration of P in the soil solution, which contains both 'dissolved' and colloidal P forms (Shand et al., 2000; Hens and Merckx, 2002; Toor and Sims, 2015). Dissolved orthophosphate is generally the main P species in solution and can be directly taken up by plant roots (Condron et al., 2005; Pierzynski et al., 2005). However, colloidal P in the size range of 1-1000 nm (Sinaj et al., 1998) may also contribute significantly to total P content in the soil solution (Haygarth et al., 1997; Shand et al., 2000; Hens and Merckx, 2001). Recent studies found that fine colloids (< 450 nm fraction) in soil water extracts consisted of nano-sized (< 20 nm) and small-sized (20 < d < 450 nm) particles with different organic matter and elemental composition (Henderson et al., 2012; Jiang et al., 2015a). Very fine nano-sized P colloids, around 5 nm are even prone to plant uptake (Carpita et al., 1979). In addition, the presence of fine colloids alters the free ionic P content in the soil solution through sorption processes (Montalvo et al. 2015). After diffusion-limited uptake depletes the free ionic P in the soil solution, these fine colloids disperse in the diffusion layer and therewith re-supply free ionic P species for roots (Montalvo et al., 2015). Because water dispersible colloids (WDCs) can be easily released from soil in contact with water (Jiang et al., 2012; Rieckh et al., 2015), they have also been suggested as model compounds for mobile soil colloids (de Jonge et al., 2004; Sequaris et al., 2013). However, little is known about the chemical composition of P species in the different-sized WDCs.

Recent studies have started to characterize natural fine colloidal P in freshwater samples and soil water extracts using asymmetric flow field flow fractionation (AF4) coupled to various detectors (e.g. ultraviolet [UV] and inductively coupled plasma mass spectrometer [ICP-MS]) for improved size fractionation of colloids and online analysis of their elemental composition (Henderson et al., 2012; Regelink et al., 2013; Gottselig et al., 2014; Jiang et al., 2015a). These analyses are increasingly combined with solution ^{31}P-nuclear magnetic resonance (NMR) spectroscopy, which offers low detection limits and can quantify different inorganic and organic P compound groups (Cade-Menun, 2005; Cade-Menun and Liu, 2014) in isolated colloidal materials (e.g. Liu et al., 2014; Jiang et al.,

74   2015a, b; Missong et al., 2016). However, we are not aware of studies that have applied these methods

75   systematically to WDCs obtained from different major reference soils. Here, we focus on the

76   comparison of Cambisols and Stagnosols. In contrast to Cambisols, Stagnosols are soils with perched

77   water forming redoximorphic features. Due to temporary water saturation and resulting oxygen

78   limitation, the reduction of iron (Fe^{III}) is accompanied by the dissolution of its oxides and hydroxides

79   (Rennert et al. 2014), and the P associated with these Fe-minerals should correspondingly be

80   redistributed in soil solution.

81   The objective of this study was to elucidate how stagnant water conditions alter the potential release of

82   different P compounds in colloidal and 'dissolved' fractions of soil solution. For this purpose, water-

83   extractable P was obtained from a transect of Cambisols to Stagnosols in a German temperate

84   grassland, and characterized using both solution ^{31}P-NMR and AF4 coupled online with UV and

85   organic carbon detector (OCD) or ICP-MS analyses.

86

87   **2. Materials and methods**

88   **2.1 Site description**

89   The grassland test site in Rollesbroich is located in the northern part of the Eifel in North Rhine-

90   Westphalia, Germany (50° 62´ N, 06° 30´ E). According to the soil map of the geological service of

91   North Rhine-Westphalia (Fig. S1), the dominant soil types on the test site are Cambisols, Stagnic

92   Cambisols, and Stagnosols (classification according to IUSS Working Group WRB, 2015). The

93   elevation along the transect generally decreases from south to north, with the highest elevation of

94   512.9 m a.s.l. at plot 1 and the lowest point of 505.1 m a.s.l. at plot 3 (Fig. S1, Table 1). The

95   catchment mean annual precipitation was 103.3 cm for the period from 1981 to 2001, and the highest

96   runoff occurred during winter seasons due to high precipitation and low evapotranspiration rates, as

97   well as overland flow due to saturation excess (Gebler et al., 2015). The topsoil samples (2-15 cm) of

98   plot 1 (S1-1, S1-2, and S1-3, Cambisol), 2 (S2, Stagnic Cambisol), and 3 (S3-1, S3-2, and S3-3,

99   Stagnosol) were taken as a representative transect across the site in early March, 2015 (Fig. S1).

100   Surface turf (0-2 cm) was removed as it contained predominantly grass roots and little mineral soil.

101   Stones and large pieces of plant material were removed by hand. All samples were sieved to < 5 mm

102   and stored at 5 °C for study.

103

104   **2.2 Water dispersible fine colloids (WDFCs) separations and AF4-UV-ICP-MS / AF4-UV-OCD**

105   **analyses**

106   The WDCs of Rollesbroich grassland soil samples with three field replicates in S1 and S3 were

107   fractionated using the soil particle-size fractionation method of Séquaris and Lewandowski (2003), but

108   with moist soils. In brief, moist soil samples (100 g of dry soil basis) were suspended in ultrapure

109   water (Mill-Q, pH: 5.5) in a soil: solution mass ratio of 1:2, and shaken for 6 h. Thereafter, 600 mL of

110   ultrapure water were added and mixed. The WDCs suspensions were collected using a pipette after 12

111   h sedimentation period. These WDCs suspensions were subsequently centrifuged for 15 min at 10,000

112    $\times g$ and filtered through 0.45 μm membranes to produce the suspension containing WDFCs sized

113   below 0.45 μm.

114   An AF4 system (Postnova, Landsberg, Germany) with a 1 kDa polyethersulfone (PES) membrane and

115   500 μm spacer was used for size-fractionation of the soil sample WDFCs. It is a separation technique

116   that provides a continuous separation of colloids; the retention time of the colloids can be converted to

117   hydrodynamic diameters of the colloids using AF4 theory or calibration with suitable standards

118   (Dubascoux et al., 2010). The AF4 was coupled online to an ICP-MS system (Agilent 7500, Agilent

119   Technologies, Japan) for monitoring of the Fe, aluminum (Al), silicon (Si), and P contents of the size-

120   separated particles (Nischwitz and Goenaga-Infante, 2012) and to OCD and UV detectors for

121   measuring organic carbon (OC). A 25 μM NaCl solution at pH 5.5, which provided good separation

122   conditions for the WDFCs, served as the carrier. The injected sample volume was 0.5 mL and the

123   focusing time was 15 min with 2.5 mL min^{-1} cross flow for the AF4-UV-OCD system while 2 mL

124   injected volume and 25 min focusing time were used for the AF4-ICP-MS system. Thereafter, the

125   cross flow was maintained at 2.5 mL min^{-1} for the first 8 min of elution time, then set to decrease

126   linearly to 0.1 mL min^{-1} within 30 min, and maintained for 60 min. It then declined within 2 min to 0

127   mL min^{-1}, and remained at this rate for 20 min to elute the residual particles.

128

Biogeosciences

Open Access

EGU

Discussions

2.3 Particle separations of WDFCs and solution ^{31}P-NMR spectroscopy analyses

129

130 The soil samples were treated as described in section 2.2 to obtain the suspension containing WDFCs

131 < 450 nm. We pooled the WDFCs suspensions of the field replicates in order to receive sufficient

132 samples for solution ^{31}P-NMR. The nano-sized colloidal particles after AF4 separation were smaller

133 than ~20 nm (approximately 300 kDa; Jiang et al., 2015a, Fig. 1). Therefore, the suspension

134 containing WDFCs < 450 nm of these three samples were separated into three size fractions: 300 kDa-

135 450 nm, 3-300 kDa, and < 3 kDa (nominally 1 nm; Erickson, 2009). The 300 kDa-450 nm particle

136 fractions were separated by passing ~600 mL of the WDFCs suspension through a 300 kDa filter

137 (Sartorius, Germany) by centrifugation. The 3-300 kDa particle fractions were subsequently isolated

138 by passing the < 300 kDa supernatant through a 3 kDa filter (Millipore Amicon Ultra) by

139 centrifugation. Finally, the final supernatant containing the < 3 kDa particles as well as the electrolyte

140 phase was frozen and subsequently lyophilized.

141 The bulk soil samples (1 g) and the three fractions of soil water extracts were respectively mixed with

142 10 mL of a solution containing 0.25 M NaOH and 0.05 M Na_2EDTA (ethylenediaminetetraacetate) for

143 4 h, as a variation of the method developed to extract soil samples for ^{31}P-NMR (Cade-Menun and

144 Preston, 1996; Cade-Menun and Liu, 2014; Liu et al., 2014). Extracts were centrifuged at 10,000 × g

145 for 30 min and the supernatant was frozen and lyophilized. Each NaOH-Na_2EDTA-treated lyophilized

146 extract, and the < 3 kDa fraction without NaOH-Na_2EDTA treatment, was dissolved in 0.05 mL of

147 deuterium oxide (D_2O) and 0.45 mL of a solution containing 1.0 M NaOH and 0.1 M Na_2EDTA

148 (Turner et al. 2007). A 10 μL aliquot of NaOD was added to the < 3 kDa fraction without NaOH-

149 Na_2EDTA treatment to adjust the pH. The prepared samples were centrifuged at 13,200 × g for 20 min

150 (Centrifuge 5415R, Eppendorf). Solution ^{31}P-NMR spectra were obtained using a Bruker Avance 600-

151 MHz spectrometer equipped with a prodigy-probe (a broadband CryoProbe which uses nitrogen [N]-

152 cooled RF coils and preamplifiers to deliver a sensitivity enhancement over room temperature probes

153 of a factor of 2 to 3 for X-nuclei from ^{15}N to ^{31}P), operating at 242.95 MHz for ^{31}P. Extracts were

154 measured with a D_2O-field lock at room temperature. Chemical shifts were referenced to 85%

155 orthophosphoric acid (0 ppm). The NMR parameters generally used were: 32 K data points, 3.6 s

156 repetition delay, 0.7 s acquisition time, 30° pulse width and 10,000 scans. Compounds were identified

157 by their chemical shifts after the orthophosphate peak in each spectrum was standardized to 6.0 ppm

158 during processing (Cade-Menun et al., 2010; Young et al., 2013). Peak areas were calculated by

159 integration on spectra processed with 7 and 2 Hz line-broadening, using NUTS software (2000 edition;

160 Acorn NMR, Livermore, CA) and manual calculation. Peaks were identified as reported earlier (Cade-

161 Menun, 2015), and by spiking a select sample with myo-inositol hexakisphosphate (myo-IHP;

162 McDowell et al., 2007).

163

164 **2.4 Statistical Analyses**

165 Elemental concentrations in bulk soils, soil water extracts, and AF4 fractograms of soil colloidal

166 particles were tested for significant differences (set to $P < 0.05$) using Sigmaplot version 12.5. A t-test

167 was conducted to determine the significance of differences among soil sites, whereas one-way

168 Repeated Measurements (RM) ANOVAs with Fisher LSD were performed with Fisher LSD post-hoc

169 test to test foridentify significant differences among soil fractions and AF4 fractograms for the

170 Cambisol and Stagnosol. Data were previously tested to meet the criteria of normal distribution and

171 homogeneity of variances; for those which had unequal variances data were $\log_{10}$- transformed before

172 statistical analyses.

173

174 **3. Results and discussion**

175 **3.1 Colloid and colloidal P distribution in different size fractions based on AF4-fractograms**

176 The AF4-UV-OCD and AF4-ICP-MS results of the WDFCs showed different OC, Si, P, Fe, and Al

177 concentrations in different-sized colloid fractions as a function of elution time (Fig. 1). The calcium

178 (Ca) results were not shown because of the generally low colloidal Ca content in these acidic soils.

179 Before the first peak, an initial small void peak occurred at 1 min (Fig. 1 D, E, F). Thereafter, three

180 different colloid-size fractions occurred individually as three peaks in the WDFCs of all samples (Fig.

181 1). The first peak of the fractograms corresponded to a particle size below 20 nm according to the

182 calibration result using latex standards (Jiang et al., 2015a). The third peak, which was eluted without

183 cross flow, contained only small amounts of residual particles or particles possibly previously attached

184 on the membrane during focus time; it had similar OC and element distributions as the second peak in

Biogeosciences

Discussions

EGU Open Access

185   all samples (Fig. 1). Therefore we considered these two fractions together as a whole. As such, the size

186   ranges from 20 to 450 nm from here onward are described as the "second size fraction".

187   For the first fraction representing nano-sized colloids of the three field sites, the OCD and UV signals

188   indicated increasing OC concentration in the order of S1 (Cambisol; Fig. 1A), S2 (Stagnic Cambisol;

189   Fig. 1B), and S3 (Stagnosol; Fig. 1C). Distinct peaks of Fe, Al, and P in the first size fraction (< 20 nm)

190   were only present in the Stagnosol (S3; Fig. 1 F), suggesting that under stagnant water conditions,

191   oxides may more readily be involved in nano-sized soil particles than under other soil conditions. In

192   contrast, negligible amount of P, Al, and Fe were detected in the first fraction of S1 and S2 (Fig. 1 D

193   and E, Table S1). While it is sometimes difficult to determine whether this peak is real or just the

194   tailing of the void signal (Fig. 1 D and E), solution ^{31}P-NMR results confirmed the presence of P in

195   this size fraction (see next section). The nano-sized colloids from the Cambisol contained OC and

196   negligible P, Fe, and Al; those from the Stagnosol contained significantly higher concentrations of OC,

197   P, Fe, and Al (Table S1). We therefore assumed that the nano-sized colloidal P forms in the Stagnosol

198   mainly consisted of OC-Fe(Al)-P associations. Nanoparticulate humic (organic matter)-Fe (Al)

199   (hydr)oxide-phosphate associations have recently been identified both in water and soil samples

200   (Gerke, 2010; Regelink et al., 2013; Jiang et al., 2015a). Our results suggest that the formation of these

201   nano-sized specific P-associations is favoured by the stagnant water conditions with high OC and

202   water contents in Stagnols but not in the other soil types along the grassland transect.

203   The second size fraction (Fig. 1 A, B, C, i.e. the small-sized colloids) contained significantly more OC

204   than the smaller nano-sized colloids for all studied soils (Table S1). Notably, the OC contents of the

205   second fraction increased in the order Cambisol < Stagnic Cambisol < Stagnosol; the UV signal

206   therein supporting the results obtained with the OC detector. The larger-sized colloids were

207   significantly richer in Al, Fe, Si, and P than the smaller-sized ones (Table S1), though again with

208   differences among subsites: now the stagnic Cambisol showed the largest Fe, Al, and Si contents in

209   the second fraction, as if there were a gradual change from low WDFC release in the Cambisol to the

210   formation of larger WDFC in the stagnic Cambisol and finally to the formation of smaller WDFC in

211   the Stagnosol. Though this trend warrants verification by more sites, it appeared at least as if the

212   increasing oxygen limitation from Cambisols via stagnic Cambisols to Stagnosols promoted an

213   increasing formation of small C-rich P-containing nanoparticles with additional contributions from Fe-

214   and Al-containing mineral phases. Stagnosols like S3 are characterized by a dynamic reduction regime

215   with dissolution of reactive Fe oxides (Rennert et al. 2014), which leads to a decrease in the content of

216   Fe oxides in the second colloidal fraction (Table S1). Correspondingly, the dissolution of Fe oxides in

217   the second fraction under stagnant water may also liberate OC from the organo-Fe mineral

218   associations, thus releasing OC to the nano-sized first fraction. This could be an additional reason for

219   the higher concentration of OC in the first peak of S3 (Table S1), apart from a generally slower

220   degradation of organic matter under limited oxygen supply (Rennert et al. 2014). Hence, the AF4

221   results indicated that the composition and distribution of particulate P varied among the different-sized

222   colloidal particles, and that its properties were impacted by the soil type and related properties.

223   However, AF4-ICP-MS results do not provide information about the elemental concentrations of the

224   'dissolved' P fraction of these grassland soils.

225

226   **3.2 Soil total, colloidal and dissolved P contents based on fractionation by filtration**

227   Soil water extracts < 450 nm, < 300 kDa, and < 3 kDa were obtained by filtration for determination of

228   total elemental contents by ICP-MS analysis. Data did not have to be pooled for these analyses; as

229   such, we could test statistical differences. We considered the soil water extract < 3 kDa in this paper to

230   be the 'dissolved' fraction. Significant differences ($p < 0.05$) were ascertained for elevated

231   concentrations of TOC, total P and Ca, as well for lower concentrations of total Al and Fe in the

232   Stagnosol relative to the Cambisol (Table 1). Furthermore, the Stagnosol had significantly higher

233   concentrations of Si and P in the individual size fractions of soil water extracts (except marginally

234   significantly higher P in < 3 kDa, $p = 0.06$), as well as higher Fe and Al concentrations in < 300 kDa

235   and < 3kDa fraction than the corresponding fractions of the Cambisol (Table 2). The stagnic Cambisol

236   generally resembled the Cambisol rather than the Stagnosol in bulk soil analysis, but this was not the

237   case for the soil water extracts. This implied that the assignment of stagnic properties is related to its

238   behaviors in the colloidal particles and 'dissolved' fraction.

239   The oxygen limitation and reduction regime of the Stagnosol probably also favored the accumulation

240   of OC and dissolution of Fe oxides both in bulk soil and colloids (Rennert et al. 2014). Dissolution of

241 Fe oxides in turn results in a disaggregation of colloidal particles (Jiang et al., 2015a). As the released

242 oxides are main carriers for P, these processes may explain why the distribution of colloidal and

243 dissolved P also changed across the different grassland soils. As Table 2 shows, large proportions of P

244 in the < 450 nm fraction of the Stagnosol were dissolved P (i.e. recovered here in the < 3 kDa fraction),

245 whereas colloidal P dominated in the Cambisol and Stagnic Cambisol.

246

3.3 Inorganic and organic P species in the different-sized soil colloidal and the 'dissolved'

247

fractions

248

249 Solution ^{31}P-NMR was used to elucidate the speciation of P in bulk soil and soil water extracts

250 separated by ultrafiltration into the size fractions 300 kDa-450 nm, 3-300 kDa, and < 3 kDa for each of

251 the three soils (Fig. 2 and S2, Table 3). The identified P included inorganic P (Pi) forms

252 (orthophosphate, pyrophosphate, and polyphosphate), and organic P (Po) in phosphonate,

253 orthophosphate monoester and diester compound classes. Phosphonates included 2-aminoethyl

254 phosphonic acid (AEP) and several unidentified peaks (Table S3). Orthophosphate monoesters

255 included four stereoisomers of inositol hexakisphosphate (*myo*-, *scyllo*-, *neo*-, and D-*chiro*-IHP),

256 diester degradation products (α-glycerophosphate, β-glycerophosphate and mononucleotides), choline

257 phosphate, and unidentified peaks at 3.4, 4.2, 4.7, 5.0, 5.3, and 5.9 ppm. Orthophosphate diesters were

258 divided into deoxyribonucleic acid (DNA) and two categories of unknown diesters (OthDi1 and

259 OthDi2, respectively). Orthophosphate, pyrophosphate, orthophosphate monoesters, and diesters have

260 also been detected in other studies of grassland, arable, and forest Cambisols and Stagnosols (e.g.,

261 Murphy et al., 2009; Turrion et al., 2010; Jarosch et al., 2015).

262 For the bulk soil samples and colloidal fractions of 300 kDa-450 nm of our soil samples,

263 orthophosphate and orthophosphate monoesters (mainly *myo*-IHP) were the main P compounds in all

264 samples (Fig. 2 and S2, Table 3 and S2). These main P compounds in these two soil fractions showed

265 similar trends among the soil samples: the proportions of Po (e.g. orthophosphate monoesters and

266 diesters) decreased in the order of Cambisol > Stagnic Cambisol > Stagnosol (Table 3). The similarity

267 in this trend for the different organic P forms can likely be attributed to similarities in the mineral

268 components of bulk soil and colloidal fractions: i.e., similar element concentrations and thus likely

269   also similar clay mineralogy, Fe oxide signature and OC content of bulk soil and respective colloid

270   fraction according to the AF4-OCD and AF4-ICP-MS results (Fig. 1 and Table S1). Orthophosphate,

271   orthophosphate monoesters and diesters are predominantly stabilized by association with these mineral

272   components (Solomon and Lehmann, 2000; Turner et al., 2005; Jiang, et al, 2015a). We assume that

273   the relatively higher proportion of orthophosphate and lower percentage of Po in the Stagnosol may be

274   attributed to the dissolution of Fe oxides, which likely released Po for mineralization (Condron et al.,

275   2005). Additionally, the higher concentrations of OC in both bulk soil (Table1) and large colloids of

276   the Stagnosol probably favored the formation of OC-Fe/Al-PO_4^{3-} complexes (see above).

277   Our study is the first to distinguish the chemical P composition in colloidal fractions of 3-300 kDa and

278   300 kDa-450 nm. We found different P speciation and distribution between these two fractions. This is

279   probably related to differences in their element composition, which are dominated by OC-P/ OC-

280   Fe(Al)-P associations in the 3-300 kDa soil fraction and by clay-Fe oxides-OC-P associations in the

281   300 kDa-450 nm size fraction (Fig. 1). Intriguingly, we did not find any Po but only Pi in the 3-300

282   kDa of all three soils (orthophosphate in Cambisol and Stagnic Cambisol, orthophosphate and

283   pyrophosphate in the Stagnosol; Table 3). Furthermore, the Stagnosol nanoparticle fraction 3-300 kDa

284   had a higher proportion of pyrophosphate than the 300 kDa-450 nm size fraction.

285   When comparing the solution ^{31}P-NMR results of the < 3 kDa soil fractions with and without NaOH-

286   Na_2EDTA treatments (Fig. 2 and Fig. S2), we observed that most of the phosphonates, orthophosphate

287   monoesters and diesters were lost after NaOH-Na_2EDTA treatment (Fig. 2 and Fig. S2). There were

288   two possible explanations: 1) 'dissolved' Po in the NaOH-Na_2EDTA solution is sensitive and easily

289   hydrolyzed to orthophosphate (Cade-Menun and Liu, 2014), or 2) in absence of NaOH-Na_2EDTA,

290   most orthophosphate was removed by adsorption on sedimentary material in the re-dissolved solution

291   after centrifugation when preparing the samples for NMR analysis (Cade-Menun and Liu, 2014),

292   resulting in elevated portions of Po in the NMR sample. The second possibility may also explain the

293   observation that there was no orthophosphate in the 'dissolved' fraction of the Cambisol without

294   NaOH-Na_2EDTA treatment (Fig. S2). Almost all the orthophosphate may have been removed with the

295   sedimentary phase due to the extremely low concentration of dissolved P in this soil. Therefore, we

296   will focus on the discussion of results obtained from the < 3 kDa soil fractions without NaOH-

297 Na$_2$EDTA treatment, as they provide better information on the origin of Po-species than the other

298 samples that received this treatment.

299 The composition of P species in the < 3 kDa soil fractions (i.e. "truly" dissolved P) differed among the

300 three soils (Table 3). The majority of P in the < 3 kDa soil fraction of the Cambisol was Po, comprised

301 mainly of phosphonates and orthophosphate monoesters. The < 3 kDa soil fraction of the Stagnic

302 Cambisol contained various P species from all compound classes, including orthophosphate,

303 orthophosphate monoesters, orthophosphate diesters, pyrophosphate, polyphosphates, and

304 phosphonates. The < 3 kDa soil fraction of the Stagnosol contained similar P species as the Stagnic

305 Cambisol, with relatively higher proportions of orthophosphate monoesters and phosphonates, but a

306 lower proportion of orthophosphate diesters (Table 3). It is worth noting that there were more species

307 of phosphonates in the < 3 kDa fraction than other fractions of each soil (Fig. 2 and S2). The larger

308 signal at ~ 21-23.5 ppm was assigned to AEP (Doolette et al., 2009; Cade-Menun, 2015), which

309 occurred in both the soil particles and the < 3 kDa fraction. However, the small signals at ~ 36-39 ppm

310 and 45-46 ppm existed only in the < 3 kDa fraction of soil samples (Fig. 2 and S2). The resonance at

311 36-39 ppm might be assigned to dimethyl methyl phosphonic acid, based on Cade-Menun (2015).

312 However, spiking experiments were not conducted to identify peaks in this region, so their specific

313 identity and origins remain unknown.

314 The solution ^{31}P-NMR results showed that P species composition in the two colloidal fractions and the

315 electrolyte phase differed among all three soil samples, with more phosphonates potentially existing in

316 the electrolyte phase. However, in the study of Missong et al. (2016), more phosphonates and

317 orthophosphate diesters were found in colloidal fractions rather than the electrolyte phase of two forest

318 Cambisols. Missong et al. (2016) used centrifugation while we used filtration to separate these particle

319 sizes and phases. Additionally, Missong et al. (2016) worked with forest soils while we worked with

320 grassland soils. McLaren et al. (2015) recently confirmed that the speciation of organic P is markedly

321 different between high (> 10 kDa) and low (< 10 kDa) molecular weight fractions of soil extracts. In

322 any case, as both colloidal aggregation and stagnant water conditions paralleled and influenced soil

323 genesis, it seems reasonable to assume that pedogenesis also affects the redistribution of different P

324 species among different P colloids and the electrolyte phase.

325

3.4 Distribution of orthophosphate monoesters and pyrophosphate

326

327 With variations in overall P species composition, the proportions of certain species of orthophosphate

328 monoesters were also differently distributed among the investigated fractions of the three soils. For

329 example, the proportion of various IHP stereoisomers (i.e. *myo*-, *scyllo*-, D-*chiro*-IHP) decreased with

330 decreasing colloid size (Table S2). This suggests that the majority of IHP was associated with soil

331 mineral particles but did not exist in the dissolved form in our soil samples. The *myo*-IHP stereoisomer

332 is the principal input of inositol phosphate to soil in the form of plant material (Turner et al. 2002) and

333 the other stereoisomers may come from plants or may be synthesized by soil organisms (Caldwell and

334 Black, 1958; Giles et al., 2015). Inositol phosphate is stabilized mainly through strong adsorption on

335 the surface of amorphous metal oxides and clay minerals (Celi and Barberis, 2007). Shang et al. (1992)

336 found *myo*-IHP sorbed onto Al and Fe oxides to a greater extent than glucose 6-phosphate. Several

337 orthophosphate monoesters such as unknown peaks at 3.4, 4.7 and 5.9 ppm were only detected in the

338 electrolyte phase of soil samples (Table S2). The differences in orthophosphate monoester species

339 distribution between soil particles and the electrolyte phase show that soil minerals such as clay

340 minerals and Fe (Al) oxides are only associated with certain species of orthophosphate monoesters

341 such as IHP, while other species of orthophosphate monoesters exist only in electrolyte phase. Further

342 research is warranted to fully understand the factors controlling Po in these different size fractions.

343 It is worth noting that although the proportion of pyrophosphate in bulk soil was very low, there was

344 more pyrophosphate in the colloidal and electrolyte phases of the Stagnic Cambisol and the Stagnosol

345 than in the Cambisol, and mostly in the electrolyte and nano-sized colloidal fraction (Table 3).

346 Pyrophosphate may be of microbial origin (Condron et al., 2005). Our former study (Jiang et al.,

347 2015b) indicated that Fe/Al oxides were not the main bonding site for pyrophosphate adsorption in

348 different-sized fractions of an arable soil. Considering that a high proportion of pyrophosphate (38.5%)

349 existed in the 3-300 kDa fraction of the Stagnosol, which contained P mainly in OC-Fe(Al)-P

350 associations (see above), it seems reasonable to assume that pyrophosphate existed as a colloidal OC-

351 Fe(Al)-pyrophosphate complex. In this regard, the accumulation of pyrophosphate may have been

352 favored by the larger OC contents in this soil (Fig. 1 C).

353

354 This study shows for the first time that P species composition varies among the electrolyte phase and

355 colloids of different size, with the specific distribution being related to the stagnic water regime of the

356 soil. It could potentially promote P availability by a mechanism that results in a loss of colloids, thus

357 providing less surface area for the immediate bonding of inorganic P to minerals, while at the same

358 time potentially releasing organic P from mineral bonding so that it is more prone to decomposition.

359 Relating the static differences in P species composition among the different soils and fractions to true

360 dynamics of P transformations, e.g., by performing controlled mesocosm experiments, now warrants

361 further attention.

362

363 **Appendix A. Supplementary data**

364 The elemental concentrations in AF4 fractograms, phosphorus spectra and species determined by

365 solution ^{31}P-NMR as well as solution ^{31}P-NMR chemical shifts of the P compounds were shown in

366 supporting information.

367

368 **Acknowledgments**

373   **References**

374   Cade-Menun, B.J., 2005. Characterizing phosphorus in environmental and agricultural samples by [31]P
375   nuclear magnetic resonance spectroscopy. Talanta, 66, 359-371.

376   Cade-Menun B.J., 2015. Improved peak identification in ^{31}P-NMR spectra of environmental samples
377   with a standardized method and peak library. Geoderma, 257-258, 102-114.

378   Cade-Menun, B.J., Carter, M.R., James, D.C., Liu, C.W., 2010. Phosphorus forms and
379   chemistry in the soil profile under long-term conservation tillage: A phosphorus-31 nuclear
380   magnetic resonance study. Journal of Environmental Quality, 39 (5), 1647-1656.

381   Cade-Menun, B.J., Liu, C.W., 2014. Solution ^{31}P-NMR spectroscopy of soils from 2005-2013, A
382   review of sample preparation and experimental parameters. Soil Science Soceity of America
383   Journal, 78, 19-37.

384   Cade-Menun, B.J., Preston, C.M., 1996. A comparison of soil extraction procedures for ^{31}P NMR
385   spectroscopy. Soil Science, 161, 770-785.

386   Caldwell, A.G., Black, C.A., 1958. Inositol hexaphosphate. II. Synthesis by soil microorganisms.
387   Soil Science Society of America Proceedings, 22, 293-296.

388   Carpita, N., Sabularse, D., Montezinos, D Delmer, D., 1979. Determination of the pore size of
389   cell walls of living plant cells. Science, 205 (4411), 1144-1147.

390   Celi, L. Barberis, E., 2007. Abiotic reactions of inositol phosphatesin soil, in: Inositol Phosphates,
391   Linking Agriculture and the Environment, edited by: Turner, B.L., Richardson, A.E., Mullaney,
392   E.J., CAB International, Wallingford, UK, 207–220, 2007.

393   Condron, L.M., Turner B.L., and Cade-Menun B.J., 2005. Chemistry and dynamics of soil organic
394   phosphorus. p. 87–121. *In* J.T. Sims, Sharpley A.N. (eds.) Phosphorus: Agriculture and the
395   Environment. ASA, CSA, SSSA. Madison, WI.

396   de Jonge, L.W., Moldrup, P., Rubæk, G.H., Schelde, K., Djurhuus, J., 2004. Particle leaching and
397   particle-facilitated transport of phosphorus at field scale. Vadose Zone Journal, 3 (2), 462-470.

398   Doolette, A.L., Smernik, R.J., and Dougherty, W.J., 2009. Spiking improved solution phosphorus-31
399   nuclear magnetic resonance identification of soil phosphorus compounds. Soil Science Soceity of
400   America Journal, 73 (3), 919-927.

401   Dubascoux, S., Le Hecho, I., Hassellöv, M., v.d. Kammer, F., Gautier, M.P. and Lespes, G., 2010.
402   Field-flow fractionation and inductively coupled plasma mass spectrometer coupling: history,
403   development and applications. Journal of Analytical Atomic Spectrometry, 25(5), 613-623.

404   Erickson, H. P., 2009. Size and shape of protein molecules at the nanometer level determined by
405   sedimentation, gel filtration, and electron microscopy. Biological Procedures Online, 11, 32–5.

406   Gebler, S., Hendricks Franssen H.J., Puetz T., Post H., Schmidt M., and Vereecken H., 2015. Actual
407   evapotranspiration and precipitation measured by lysimeters: a comparison with eddy covariance
408   and tipping bucket. Hydrol. Earth System Science, 19, 2145-2161.

409   Gerke, J., 2010. Humic (organic matter)-Al(Fe)-phosphate complexes: an underestimated phosphate
410   form in soils and source of plant-available phosphate. Soil Science, 175 (9), 417-425.
411   Giles, C.D., Lee L.G., Cade-Menun B.J., Hill J.E., Isles P.D.F., Schroth A.W., and Druschel G.K.,
412   2015. Characterization of organic phosphorus form and bioavailability in lake sediments using
413   ^{31}P NMR and enzymatic hydrolysis. Journal of Environmental Quality, 44: 882-894.
414   Gottselig, N., Bol, R., Nischwitz, V., Vereecken, H., Amelung, W., and Klumpp, E., 2014.
415   Distribution of phosphorus-containing fine colloids and nanoparticles in stream water of a forest
416   catchment. Vadose Zone Journal, 13 (7), 1-11.
417   Haygarth, P.M., Warwick, M.S., and House, W.A., 1997. Size distribution of colloidal molybdate
418   reactive phosphorus in river waters and soil solution. Water Research, 31 (3), 439-448.
419   Henderson, R., Kabengi, N., Mantripragada, N., Cabrera, M., Hassan, S., and Thompson, A., 2012.
420   Anoxia-induced release of colloid- and nanoparticle-bound phosphorus in grassland soils.
421   Environmental Science Technology, 46 (21), 11727-11734.
422   Hens, M. and Merckx, R., 2001. Functional characterization of colloidal phosphorus species in the soil
423   solution of sandy soils. Environmental Science Technology, 35 (3), 493-500.
424   Hens, M. and Merckx, R., 2002. The role of colloidal particles in the speciation and analysis of
425   "dissolved" phosphorus. Water Research, 36 (6), 1483-1492.
426   IUSS Working Group WRB. 2015. World Reference Base for Soil Resources 2014, update 2015.
427   International soil classification system for naming soils.
428   Jarosch, K.A., Doolette, A.L., Smernik, R.J., Tamburini, F., Frossard, E., and Bünemann, E.K., 2015.
429   Characterisation of soil organic phosphorus in NaOH-EDTA extracts: A comparison of ^{31}P NMR
430   spectroscopy and enzyme addition assays. Soil Biology and Biochemistry, 91, 298-309.
431   Jiang, C., Séquaris, J.-M., Vereecken, H., and Klumpp, E., 2012. Effects of inorganic and organic
432   anions on the stability of illite and quartz soil colloids in Na-, Ca- and mixed Na–Ca systems.
433   Colloids and Surfaces A: Physicochemical and Engineering Aspects, 415 (0), 134-141.
434   Jiang, X., Bol, R., Nischwitz, V., Siebers, N., Willbold, S., Vereecken, H., Amelung, W., and Klumpp,
435   E., 2015a. Phosphorus containing water dispersible nanoparticles in arable soil. Journal of
436   Environmental Quality, 44 (6), 1772-1781.
437   Jiang, X., Bol, R., Willbold, S., Vereecken, H., and Klumpp, E., 2015b. Speciation and distribution of
438   P associated with Fe and Al oxides in aggregate-sized fraction of an arable soil. Biogeosciences,
439   12 (21), 6443-6452.
440   Liu, J., Yang, J., Liang, X., Zhao, Y., Cade-Menun, B.J., and Hu, Y., 2014. Molecular speciation of
441   phosphorus present in readily dispersible colloids from agricultural soils. Soil Science Society of
442   America Journal, 78 (1), 47-53.
443   McDowell, R.W., Cade-Menun, B., and Stewart, I., 2007. Organic P speciation and pedogenesis:
444   analysis by ^{31}P nuclear magnetic resonance spectroscopy. European Journal of Soil Science, 58,
445   1348-1357.

446   McLaren, T.I., Smernik, R.J., McLaughlin, M.J., McBeath, T.M., Kirby, J.K., Simpson, R.J., Guppy,
447   C.N., Doolette A.L., and Richardson, A.E., 2015. Complex forms of soil organic phosphorus – A
448   major component of soil phosphorus. Environmental Science Technology, 49, 13238-13245.

449   Missong, A., Bol, R., Willbold, S., Siemens, J., and Klumpp, E., 2016. Phosphorus forms in forest soil
450   colloids as revealed by liquid-state ^{31}P-NMR. Journal of Plant Nutrition and Soil Science, 179 (2),
451   159-167.

452   Montalvo, D., Degryse, F., and McLaughlin, M.J., 2015. Natural colloidal P and its contribution to
453   plant P uptake. Environmental Science Technology, 49 (6), 3427-3434.

454   Murphy, P.N.C., Bell, A., and Turner, B.L., 2009. Phosphorus speciation in temperate basaltic
455   grassland soils by solution ^{31}P NMR spectroscopy. European Journal of Soil Science, 60, 638-651.

456   Nischwitz, V., and Goenaga-Infante, H., 2012. Improved sample preparation and quality control for
457   the characterisation of titanium dioxide nanoparticles in sunscreens using flow field flow
458   fractionation on-line with inductively coupled plasma mass spectrometry. Journal of Analytical
459   Atomic Spectrometry, 27 (7), 1084-1092.

460   Pierzynski, G.M., McDowell, R.W., and Sims, J.T., 2005. Chemistry, cycling and potential movement
461   of inorganic phosphorus in soils. p. 53–86. *In* J.T. Sims, and A.N. Sharpley (eds.) Phosphorus:
462   agriculture and the environment. ASA, CSA, SSSA. Madison, WI.

463   Regelink, I.C., Koopmans, G.F., van der Salm, C., Weng, L., and van Riemsdijk, W.H., 2013.
464   Characterization of colloidal phosphorus species in drainage waters from a clay soil using
465   asymmetric flow field-flow fractionation. Journal of Environmental Quality, 42 (2), 464-473.

466   Rennert, T., Händel, M., Höschen, C., Lugmeier, J., Steffens, M., and Totsche, K.U., 2014. A
467   NanoSIMS study on the distribution of soil organic matter, iron and manganese in a nodule from
468   a Stagnosol. European Journal of Soil Science, 65 (5), 684-692.

469   Rieckh, H., Gerke, H.H., Glæsner, N., Kjaergaard, C., 2015. Tracer, dissolved organic carbon, and
470   colloid leaching from erosion-affected arable hillslope soils. Vadose Zone Journal, 14, 1539-1663.

471   Sequaris, J.M., Klumpp, E., and Vereecken, H., 2013. Colloidal properties and potential release of
472   water -dispersible colloids in an agricultural soil depth profile. Geoderma, 193-194, 94-101.

473   Séquaris, J.M., and Lewandowski, H., 2003. Physicochemical characterization of potential colloids
474   from agricultural topsoils. Colloids and Surfaces A: Physicochemical and Engineering Aspects,
475   217 (1-3), 93-99.

476   Shand, C.A., Smith, S., Edwards, A.C., and Fraser, A.R., 2000. Distribution of phosphorus in
477   particulate, colloidal and molecular-sized fractions of soil solution. Water Research, 34 (4), 1278-
478   1284.

479   Shang, C., Stewart, J.W.B., and Huang, P.M., 1992. pH effect on kinetics of adsorption of organic and
480   inorganic phosphates by short-range ordered aluminum and iron precipitates. Geoderma, 53 (1),
481   1-14.

482   Sinaj, S., Machler, F., Frossard, E., Faisse, C., Oberson, A., and Morel, C., 1998. Interference of
483   colloidal particles in the determination of orthophosphate concentrations in soil water extracts.
484   Communications in Soil Science and Plant Analysis, 29 (9-10), 1091-1105.

485   Solomon, D. and Lehmann, J., 2000. Loss of phosphorus from soil in semi-arid northern Tanzania as a
486   result of cropping: evidence from sequential extraction and ^{31}P-NMR spectroscopy. European
487   Journal of Soil Science, 51, 699-708.

488   Toor, G.S., and Sims, J.T., 2015. Managing phosphorus leaching in mid-Atlantic soils: importance
489   of legacy sources. Vadose Zone Journal, 14 (12), 1-12.

490   Turner, B. L., Cade-Menun, B. J., Condron, L. M., and Newman, S., 2005. Extraction of soil organic
491   phosphorus. Talanta, 66, 294-306.

492   Turner, B., Condron, L., Richardson, S., Peltzer, D., and Allison, V., 2007. Soil organic phosphorus
493   transformations during pedogenesis. Ecosystems, 10 (7), 1166-1181.

494   Turner, B.L., Papházy, M.J., Haygarth, P.M., and McKelvie, I.D., 2002. Inositol phosphates in the
495   environment. Philosophical Transactions of the Royal Society B Biological Sciences, 357 (1420),
496   449-469.

497   Turrion, M.B., Lafuente, F., Aroca, M.J., López, O., Mulas, R., and Ruipérez, C., 2010.
498   Characterization of soil phosphorus in a fire-affected forest Cambisol by chemical extractions and
499   ^{31}P-NMR spectroscopy analysis. Science of the Total Environment, 408 (16), 3342-3348.

500   Vance, C.P., Uhde-Stone, C., and Allan, D.L., 2003. Phosphorus acquisition and use: critical
501   adaptations by plants for securing a nonrenewable resource. New Phytologist, 157 (3), 423-447.

502   Young, E.O., Ross, D.S., Cade-Menun, B.J., Liu, C.W., 2013. Phosphorus speciation in riparian soils:
503   A phosphorus-31 nuclear magnetic resonance spectroscopy and enzyme hydrolysis study. Soil
504   Science Society of America Journal, 77 (5), 1636-1647.

Biogeosciences
Discussions

Open Access

Table 1 General soil characteristics and concentrations of dissolved organic carbon (TOC), total Fe, Al, P, Ca, and Si in bulk S1 (Cambisol), S2 (Stagnic Cambisol), and S3 (Stagnosol). The uppercase letters indicate significant differences among soil sites (significant difference of soil site 1 and 3 was tested by t-test, $p < 0.05$).

Soil	pH^{IV}	Water content (%)	Elevation (m a.s.l.)	TOC (g kg^{-1})	Fe* (g kg^{-1})	Al (g kg^{-1})	P (g kg^{-1})	Ca (g kg^{-1})	Si (g kg^{-1})
S1[I]	4.90±0.12a	46.5±2.9	512.9	35.6±2.3a*	23.0±1.1a*	52.6±2.9a	1.2±0.1a	1.8±0.1a	320±7.6
S2[II]	4.90	45.3	507.5	35.8	24.0±0.4	54.0±2.0	1.3±0.1	1.8±0.03	320±7.0
S3[III]	5.36±0.20b	59.0±7.6	505.1	71.1±15.1b*	12.8±0.4b*	38.7±1.1b	1.8±0.4b	3.0±0.5b	312±12.1

[I] The mean of sample S1-1, S1-2, and S1-3 ± standard deviation.

[II] The mean of three replicate sample S2 ± standard deviation.

[III] The mean of sample S3-1, S3-2, and S3-3 ± standard deviation.

[IV] The mass ratio of soil : water = 1:2.5.

* Data were log transformed before t-test analyses because of unequal variances.

Biogeosciences Discuss., doi:10.5194/bg-2016-434, 2016
Manuscript under review for journal Biogeosciences
Published: 14 October 2016

Table 2 Concentrations of P, Al, Fe, and Si in soil water extracts < 450 nm, < 300 kDa, and < 3 kDa, respectively. Different lowercase and uppercase indicate significant differences among soil sites and soil fractions, respectively (significant difference of soil sites 1 and 3 was tested by t-test, One Way RM ANOVA for soil fractions with Fisher LSD post-hoc test, $P <0.05$).

Soil	TOC (g kg⁻¹)	P (mg kg⁻¹)			Al (mg kg⁻¹)			Fe (mg kg⁻¹)			Si (mg kg⁻¹)		
	< 450 nm	<450nm	<300kDa	<3kDa	<450nm	<300kDa	<3kDa	<450nm	<300kDa	<3kDa	<450nm	<300kDa	<3kDa
S1[I]	0.18	0.3±0.1a*	0.2±0.2a*	0.1±0.1	2.0±0.4A°	0.6±0.0[a]aB°	0.6±0.0[a]aB°	2.1±0.5A	0.2±0.0[a]aB	0.2±0.0[a]a*B	8.1±0.6aA	6.8±0.3aB	6.6±0.4aB
S2[II]	0.17	1.3±0.9	0.5±0.6	0.4±0.3	7.3±0.3	1.1±0.2	1.1±0.2	9.2±0.5	0.4±0.1	0.4±0.1	14.1±0.5	7.3±0.0[a]	7.8±0.8
S3[III]	0.23	4.4±2.0b*	3.3±2.7b*	4.1±2.6	4.1±3.1	0.7±0.1b	0.7±0.0b	4.6±3.3	0.4±0.1b	0.5±0.1b*	14.6±1.3b	10.6±2.1b	11.4±2.5b

[I] The mean of sample S1-1, S1-2, and S1-3 (Cambisol) ± standard deviation.

[II] The mean of three replicate extracts of sample S2 (Stagnic Cambisol) ± standard deviation.

[III] The mean of sample S3-1, S3-2, and S3-3 (Stagnosol) ± standard deviation.

[a] Standard deviation of 0.0 means value <0.05.

*Data were log transformed before t-test analyses because of unequal variances.

°Data were log transformed before One Way RM ANOVA analyses because of unequal variances.

528 Table 3 the proportion (%) of phosphorus species[a] determined by solution ^{31}P-NMR for the different
529 soil fractions of S1 (Cambisol), S2 (stagnic Cambisol), and S3 (Stagnosol).

Soil fractions	Pi	Po	Ortho-P	Pyro-P	poly	P-mono	P-mono*	P-diest	P-diest*	Phon-P
										----%----------------
S1 bulk	43.4	56.6	41.2	1.5	0.7	52.9	44.5	2.2	10.6	1.5
S2 bulk	47.8	52.2	46.4	0.9	0.5	48.6	43.7	1.4	6.3	2.2
S3 bulk	63.7	36.3	63.0	0.2	0.5	31.2	27.0	1.5	5.7	3.6
S1 300 kDa-450 nm	22.8	77.2	22.8	-[y]	-	56.7	49.5	11.1	18.3	9.4
S2 300 kDa-450 nm	56.8	43.2	53.1	1.0	2.7	29.9	26.9	5.2	8.2	8.1
S3 300 kDa-450 nm	70.2	29.8	59.7	9.2	1.3	24.2	19.9	2.8	7.1	2.8
S1 3-300 kDa	100	-	100	-	-	-	-	-	-	-
S2 3-300 kDa	100	-	100	-	-	-	-	-	-	-
S3 3-300 kDa	100	-	61.5	38.5	-	-	-	-	-	-
S1 < 3 kDa	13.5	86.5	-	-	13.5	26.9	26.9	1.9	1.9	57.7
S2 < 3 kDa	21.3	78.7	9.5	5.1	6.7	29.3	13.8	24.2	34.6	25.2
S3 < 3 kDa	22.2	77.8	8.8	6.0	7.4	29.4	27.4	8.2	10.2	40.2

530 [a] inorganic P (P$_i$), organic P (P$_o$), orthophosphate (Ortho-P), pyrophosphate (Pyro-P), polyphosphate
531 (poly), orthophosphate monoesters (P-mono), orthophosphate diesters (P-diest), phosphonates (Phon-
532 P). * recalculation by including diester degradation products (α glycerophosphate, β glycerophosphate,
533 and mononucleotides) with P-diest rather than P-mono (Liu et al. 2014; Young et al. 2013). [y] below
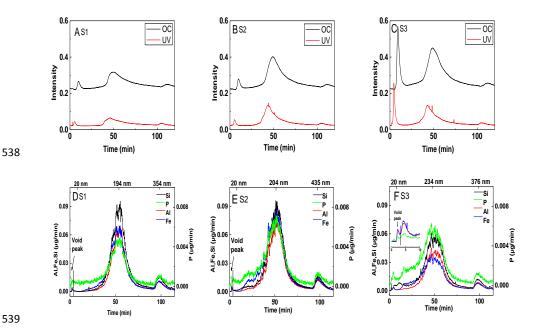534 detection limit.
535

536

537

Fig. 1 Asymmetric flow field-flow fractionation (AF4) fractograms of water dispersible fine colloids (WDFCs) of S1, S2, and S3. The fractograms show the organic carbon (OC) and ultraviolet (UV) signal intensities (A, B, and C) and the Fe, Al, P, and Si mass flow (D, E, and F) monitored by inductively coupled plasma mass spectrometer (ICP-MS) of S1 (Cambisol), S2 (Stagnic Cambisol), and S3 (Stagnosol). The sizes of peaks were according to the AF4 result of sulfate latex standard particles and dynamic light scattering results. The slight retention time shift between OCD and UV is due to the internal volume between these two detectors.
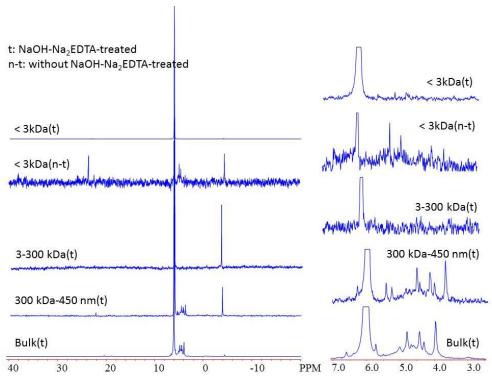
555

Fig. 2 Solution phosphorus-31 nuclear magnetic resonance spectra of NaOH–Na$_2$EDTA extracts of

bulk soil, 300 kDa-450 nm, 3-300 kDa and < 3 kDa fractions in soil water extracts < 450 nm of S3

(Stagnosol).

556

557

558

559

560